A hybrid stochastic Lagrangian – cellular automata framework for modelling fire propagation in inhomogeneous terrains

Epaminondas Mastorakos [a,*], Savvas Gkantonas [a], Georgios Efstathiou [a], Andrea Giusti [b]

[a] *Department of Engineering, University of Cambridge, Cambridge, UK*
[b] *Mechanical Engineering Department, Imperial College London, UK*

Abstract

A stochastic model motivated by the Lagrangian transported probability density function method for turbulent reacting flows and the cellular automata approach for forest fires was put together to simulate propagation of fires in terrains with inhomogeneous composition. In contrast to the usual cellular automata models for fires where the probability of ignition is prescribed, here the ignition of cells is determined by a random walk that mimics turbulent convection and diffusion of the hot gases and firebrands from upwind and neighbouring fire fronts. Radiation is also included. The model is aimed at speed of computation while approximating the key physics through only a few terrain-related inputs and tunable parameters representing fire intensity, hot gas and ember decay timescales, cell ignition delay and local turbulence. These parameters were calibrated against controlled fire experiments and the model was then used to give reasonable predictions for fires of increasing complexity. The presented framework allows improvements for more accurate representation of the flammable material characteristics, fire-induced flow modifications, and most other phenomena present in fires, hence providing an extendable and simple yet physically-realistic novel modelling approach.
© 2022 The Author(s). Published by Elsevier Inc. on behalf of The Combustion Institute.
This is an open access article under the CC BY-NC-ND license
(http://creativecommons.org/licenses/by-nc-nd/4.0/)

Keywords: Fire propagation; Cellular automaton; Random walk; Wildland-urban interface; Mati attica

1. Introduction

The problem of wildfire propagation and fires in the wildland-urban interface (WUI) has been extensively reviewed; for example, see Refs. [1–10]. A forest fire in general propagates due to convection of the hot gases, firebrands, and radiation. The timescales and spatial extent of these processes depend on various parameters that can be separated as belonging to the fire front, to the unburnt area, or to the wind, broadly speaking. Such parameters include the wind velocity and its fluctuations, the

intensity of the fire front, and the type of burning material, while the ignitability of the neighbouring area depends on the type of flammable material there and on the "reception" of information from the fire front, which includes the effects of slope and radiative shielding. This conceptual separation of the physical processes involved in fire propagation into "emitting" (i.e., the characteristics of the fire front), "receiving" (i.e., the characteristics of the still unburnt material), and the "bridge" between the two (i.e., the wind, radiation, firebrand motion) motivates the modelling framework proposed in this paper. Such a distinction allows the inclusion of fine-grained terrain information and enables the development of physics-based models for the probability of fire reaching a certain point.

For the very dangerous case of fires reaching buildings and WUI fires, models need to be adapted to account for non-flammable regions (e.g., plots of land that do not contain flammable vegetation), tall buildings that may block the fire in particular directions, and crown fires that may go over houses and spread in neighbouring houses and gardens. Therefore, tree-scale and house-scale information may be necessary for accurate predictions. The availability of such models can help with the development of evacuation strategies and assist real-time decisions [11]. Models can also be used to estimate the destructive potential of a fire, therefore assisting the design of fire fighting systems and guiding landscaping choices to reduce the risk of uncontrolled fire propagation. In addition, the stochastic behaviour of such a fire (e.g., the "patchy" nature of the burnt region) is of interest. It is difficult to include such granularity of information and stochasticity in Eulerian descriptions due to the grid resolution needed to resolve strong gradients in properties and due to the fact that often such models solve for the average behaviour only.

In this paper, a stochastic model borrowed from turbulent flame propagation in complex flow fields with relevance to the ignition of gas turbines [12], which includes local phenomena such as fuel availability and quenching, is adapted and extended to simulate propagation of forest and WUI fires. It also borrows ideas from the cellular automata approach (for example, Refs. [13–15]) that separates the area into cells, each having its own properties and where propagation is modelled by a prescribed probability of ignition. Here, this probability is explicitly calculated through the random walk of hot gases, firebrands and radiation. The resulting model provides a framework with only a few parameters, which can be determined from material burning behaviour or from calibration against controlled fire experiments and then used for a wide range of grassland, crown, and WUI fires. The key purpose of the model is ease of operation and speed of calculation while maintaining fidelity to the key physical processes. It provides "placeholders" for future inclusion of more refined physical modelling of the various processes that can be used to provide the values of the model's key parameters. The model is denoted by the acronym FireSPIN, following the approach of Ref. [12] where stochastic particles are integrated forward in time, but this time applied to fires rather than ignition of combustors.

The objectives of this paper are: (i) to develop a common framework of modelling wind-driven forest and WUI fires focusing on terrain inhomogeneity and stochastic behaviour; (ii) to demonstrate a methodology on how the model's parameters can be selected based on the fire and flammable material characteristics; and (iii) to demonstrate its performance for some WUI fires. The key features of the proposed framework are presented in Section 2, followed by calibration against experiments and evaluation for a real WUI fire. Possible extensions are also discussed.

2. Methods

2.1. The basic idea

The model is aimed mostly at wind-driven fires. It borrows ideas from the cellular automata approach [13] and in particular those models where the propagation rules are explicitly related to the underlying physical processes [14,16–18]. Here, a stochastic random walk of *virtual particles* (hot fluid particles or embers) is developed to account for convection by the mean flow and turbulent dispersion of the flame's hot gases and firebrands that are emitted from a burning cell. An ignition delay timescale is introduced to account for the ignitability of the cell receiving these particles. To account for dilution and temperature decay, and hence loss of their capability to ignite neighbouring cells, a first-order decay of a normalised temperature of each of these virtual particles is included, so that below a threshold these particles cannot ignite unburnt cells any more. If an unburnt cell receives a burning particle, its ignition is modelled by the cell emitting its own particles, one or more, simultaneously or spread over a burning duration, after a delay to account for initial fire growth. A simplified ray tracing method is used for radiative heat transfer, mostly added for completeness. The resulting rate of fire spread depends on the values of a few parameters that are found by calibration, while vegetation-specific properties are input through case-specific constants.

In wind-driven fires, the fire front propagation speed, S_f, is very important. A rule of thumb is that $S_f \approx 0.1 U_w$, where U_w is the 10-m wind speed (i.e., the time-averaged wind speed at a height of 10 m above ground), but this estimate comes with a large margin of error [5]. Empirical expressions [4] for the ratio S_f/U_w include the canopy bulk density and moisture content. Other important trends are

that: (i) S_f/U_w decreases as moisture increases; (ii) S_f increases with materials that produce many firebrands [10]. The model aims to reproduce S_f and to include spatial information on local flammability and burn time.

2.2. Governing equations

In this paper, a 2D version of the model is presented, but it is straightforward to extend the proposed framework to 3D. The governing equations for the random walk of the convection fire particles are:

$$\frac{\mathrm{d}Y_{\mathrm{st,p}}}{\mathrm{d}t} = -\frac{Y_{\mathrm{st,p}}}{\tau_{\mathrm{mem}}}; \tag{1}$$

$$\mathrm{d}X_{i,p} = F_l \, U_{i,p} \, \mathrm{d}t \ \text{ where } \ i = 1, 2; \tag{2}$$

$$\mathrm{d}U_{i,p} = -\frac{(2 + 3C_0)}{4} \frac{u'}{L_t}(U_{i,p} - U_{w,i})\mathrm{d}t + (C_0 \varepsilon \mathrm{d}t)^{1/2}\mathcal{N}_i. \tag{3}$$

The random walk above is based on the well-known Lagrangian description of turbulent dispersion [19], supplemented with a simple decay of the scalar $Y_{\mathrm{st,p}}$ following the Lagrangian PDF method for reacting flows [19]. In Eq. (3), u' and L_t are the turbulent velocity fluctuations and integral lengthscale respectively, which imply $\varepsilon = u'^3/L_t$. C_0 is a constant close to 2, and $\mathcal{N}_i$ is a normally-distributed random variable with zero mean and unit variance. $U_{w,i}$ is the component of the wind speed in the $i-$th direction and $U_{\mathrm{i,p}}$ is the current component velocity of the particle. For the atmospheric boundary layer and since here we are focusing on transport close to the ground, the following values are used: (i) $u' = AU_w$ with $A = 0.2$–0.4. (ii) L_t is taken as the height of the fire emitting the particles (consistent with the choice that in turbulent boundary layer theory the integral lengthscale is taken as the distance from the wall), and may have values 10–40 m or more. (iii) U_w is the wind speed at 10 m above ground, for consistency with the literature of wind-driven fires.

It is known that $S_f < U_w$. This is because (i) each flammable material (building, tree, bush etc.) takes time to ignite; (ii) firebrands have finite mass and lifetime; (iii) radiation decays with distance; and (iv) hot gases from the fire front get diluted. To partly account for these phenomena, in the current model, the convection fire particles move in a random walk, and their new position is scaled by a factor F_l. This parameter will come from calibration (or, for firebrands, explicit trajectory and temperature models [10,20]).

The scalar $Y_{\mathrm{st,p}}$ denotes the particle's "burning status": this is a quantity between 0 and 1, indicating whether the particle is hot ($Y_{\mathrm{st,p}} = 1$) and hence

capable of igniting further fire, or colder than a critical value ($Y_{\mathrm{st,p}} < Y_{\mathrm{lim}}$) and hence not capable of igniting further fire. This threshold could be chosen according to the minimum ignition temperature of the receiving flammable material, and can hence be connected to the properties of the unburnt cell. Here, $Y_{\mathrm{lim}} = 0.2$ is used, rationalised considering the following example. If initially a convection particle is at, say, 2000 K, it will not ignite a fire further after its temperature falls below 400 K taken as a typical ignition temperature. This parameter can be estimated through more sophisticated modelling of the decay rate of the firebrand or dilution of the hot gases. The results are not very sensitive to Y_{lim} when it remains in the reasonable range 0.1–0.3.

The quantity τ_{mem} determines the decay rate and is a parameter of the model. If this timescale is large, the particle has far-reaching potential to ignite a fire (i.e., it can cause spot fires far away from its generation), while if it is small it quickly decays and does not cause ignitions elsewhere. This parameter can also be thought of to depend on the cell's intensity of fire and hence can be made a function of the fire that emitted this particular particle. τ_{mem} does not need to be the same for all particles. In addition, one can easily develop a more rational approach for mimicking the particle's decay, e.g., by a dedicated energy balance. The present framework allows for that, however this is not implemented here and a constant value of order of a few tens of seconds is used.

The random walk for the radiation particles obeys:

$$\begin{aligned}\mathrm{d}X_{1,p} &= L_r \cos(\phi_r) \\ \mathrm{d}X_{2,p} &= L_r \sin(\phi_r)\end{aligned} \ , \text{ where } \ \phi_r = \xi. \tag{4}$$

In Eq. (4), ξ is a uniformly distributed random variable between 0 and 2π. The radiation particle's $Y_{\mathrm{st,p}}$ follows Eq. 1 but with a decay timescale $\tau_{\mathrm{mem}} = L_r/S_{\mathrm{f,0}}$, where $S_{\mathrm{f,0}}$ is the no-wind propagation speed taken here as constant and equal to 0.1 m/s, but it could be a function of space or local conditions [21]. $L_r = 10$ m was used here.

2.3. Spatial discretisation

The region can be split in cells of arbitrary shape (a square grid was used here). In a simulation of a fire propagating in a WUI, it is expected that each cell may represent each plot of land, houses or groups of houses with their gardens, roads, squares or sports fields. The flammable materials (vegetation or buildings) are characterised by a few model choices. First, the ignition delay time, τ_{ign}: this is a timescale that determines the time difference between initiation of the fire (e.g., by an ember) and self-sustaining burning. It depends on the type of vegetation and the prevailing humidity, and is a key input to the model. This timescale can be separately calculated through approaches such as CFD or extracted from observations [22]. For large dry trees,

we may expect this parameter to be in the order of a few tens of seconds. Second, the number of new particles emitted and their phasing: in the present implementation only one new particle is emitted at $t = \tau_{ign}$ after the cell received a burning particle. However, the framework allows an arbitrary number of particles to be emitted, each following their own random walk, at various times hence mimicking long-burning fires such as wooden houses. Note that since the model is meant to be run numerous times, the number of particles emitted per cell and the number of realisations provide complementary routes to access the full sample space of fire front evolution.

2.4. The algorithm

The algorithm operates as follows:

1. For one or more cells that mark the fire initiation point, launch their particles by setting (i) $Y_{st,p} = 1$; and (ii) $dU_{i,p}$ from Eq. (3).
2. Track the particles that have $Y_{st,p} > Y_{lim}$ for a timestep Δt according to Eqs. 1–3.
3. If a cell is visited by a "live" particle (i.e., if $Y_{st,p} > Y_{lim}$), start the cell's clock.
4. When the cell's clock shows a time greater than the cell's τ_{ign}, the cell emits all its particles either simultaneously or spread over a duration by setting their $Y_{st,p} = 1$. In order to account for natural fluctuations in τ_{ign} even in the case of uniform vegetation, a small random component of 10–20% is built-in, but the results are not sensitive to this choice.
5. Continue tracking the position and $Y_{st,p}$ of all particles that have $Y_{st,p} > Y_{lim}$.

Counting how many cells ignited constitutes one of the main results of the algorithm concerning the fire spread. Visualising the motion of the particles is another main result.

2.5. Summary of model parameters

Given a wind speed U_w and a given underlying turbulence field (i.e., u' and L_t), there are five main parameters in the present fire propagation model: (i) τ_{mem}; (ii) τ_{ign}; (iii) F_l; (iv) L_r; and (v) Y_{lim}. By suitable choice of these parameters, to be determined through analysis of the individual sub-processes or calibration against experiments, a wide range of fires can be modelled. In particular: (i) τ_{mem} is of $O(10)$ s but can be more accurately determined by a simple analysis of the unsteady diffusion equation; (ii) τ_{ign} is critical for the numerical value of the resulting S_f and comes from calibration against well-controlled experiments or empirical data; (iii) F_l will come from calibration against experiments in wind-driven fires; (iv) L_r is determined by examination of fire propagation in the absence of wind; and (v) Y_{lim} can be fixed from a simplified analysis

based on a typical flame temperature and a typical minimum ignition temperature. The particular choices used here are given in Table 1 and discussed in the Results section in connection with the particular fire to be modelled.

3. Results and discussion

The model is assessed in this Section through the examination of a few canonical problems and some fire examples from the literature that include fires in grassland and a devastating fire in an pine tree-laden urban area in Mati, Greece, 23 July 2018.

3.1. Canonical problems

The behaviour of the model in the situation of no wind, uniform wind, ignition from a point, ignition from a line, and the structure of the fire front far from the ignition are first assessed. We also consider a problem with regions that are non-flammable. The key quantities of interest are: (i) the overall shape of the flame and its speed of propagation under various wind speeds; (ii) the sensitivities of these to the values of the parameters.

If $U_w = 0$, the fire propagates by radiation only. In the literature, this speed is mentioned as the *no-wind rate of spread*, R_0, and depends on the vegetation only. In the present model, the radiation-driven propagation is determined by the model constants L_r and τ_{ign}, with τ_{mem} and F_l not affecting radiative propagation. In Fig. 1, the evolution of the fire particles at various times is shown. The colour of the points corresponds to each particle's $Y_{st,p}$ and starts from zero if the cell has not been touched yet by radiation from the neighbours and becomes unity the moment the cell is ignited. It is evident that the fire propagates in a front that has some stochasticity, but is broadly circular, as expected. The R_0 from Fig. 1 is around 0.06 m/s, which is a reasonable value for large pine trees [21], suggesting that the choice of parameters above is sensible.

In Fig. 1c-d, a wind of 10 m/s is used. The following observations can be made. First, the fire moves predominantly in the wind direction, as expected. If the wind speed is low enough, some upwind propagation is possible (not shown here). Second, the side flanks are burning less vigorously and the propagation in the cross-wind direction is smaller than in the wind direction. Third, the thickness of the fire front is of the order of 10 m. Finally, the fire front is moving at a speed S_f of about 1.2 m/s and 1.5 m/s for $\tau_{mem} = 10$ s and 30 s respectively, giving a reasonable range of the ratio S_f/U_w. Note how an increase in the particle "memory", representing the timescale beyond which gases or firebrands cannot ignite unburnt cells, increases the fire front speed, as expected.

Fig. 2 contains results from a line ignition case, to give a statistically-uniform fire front in the $y-$direction. These simulations also contain large
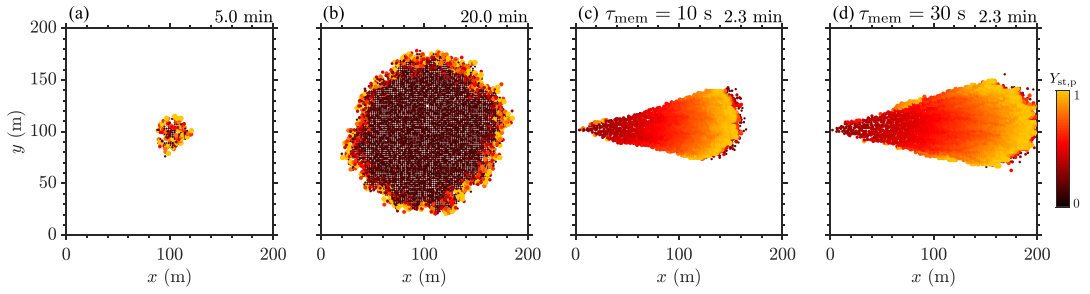
Fig. 1. Fire particles, sized and coloured by their $Y_{st,p}$, in the case of point ignition at the domain centre with uniform vegetation and no wind after (a) 5 min and (b) 20 min, and at 2.3 min after point ignition at $(x, y) = (0, 50)$ with uniform vegetation and wind with (c) $\tau_{mem} = 10$ s and (d) $\tau_{mem} = 30$ s. Parameters are taken from Table 1 unless stated otherwise.
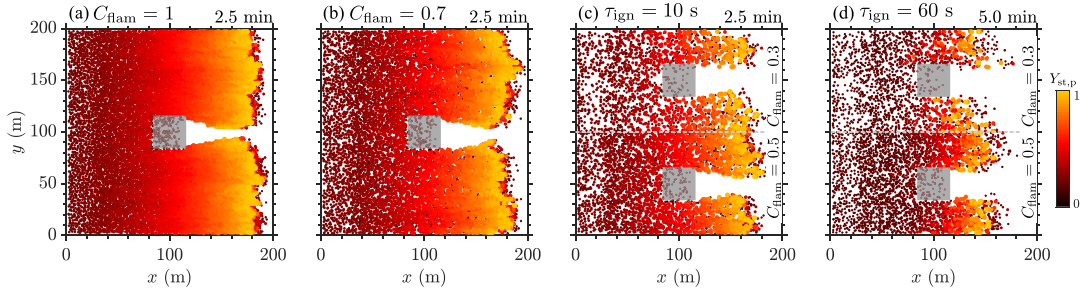

Fig. 2. Fire particles, sized and coloured by their $Y_{st,p}$ at the indicated time from line ignition at $x = 0$. 32×32 m buildings are included. (a) Uniform vegetation with one building at 2.5 min after ignition. (b) Same as (a) but with 70% coverage ratio with flammable cells. (c)-(d) Upper half and lower half have the indicated coverage ratio and (c) τ_{ign}=10 s and (d) τ_{ign}=60 s. Parameters are taken from Table 1 unless stated otherwise.

Table 1
Parameters used in the various cases. In all simulations in this paper, the grid was uniform with size Δ. C_{flam} is the fraction of the domain cells that are flammable.

Figure	Domain (km)	Δ (m)	C_{flam}	U_w (m/s)	A	L_t (m)	L_r (m)	τ_{mem} (s)	τ_{ign} (s)	F_l	Y_{lim}
Figs. 1a–b	0.2×0.2	2	1	0	–	–	10	–	10	–	0.2
Figs. 1c–d	0.2×0.2	2	1	10	0.3	50	10	10–30	10	0.15	0.2
Fig. 2	0.2×0.2	2	0.3–1	10	0.3	50	10	10	10–60	0.15	0.2
Fig. 4	0.2×0.2	2	0.91	7.7	0.2	10	10	10	6.2	0.1–0.2	0.2
Fig. 6	7.5×7.5	25	0.65	25	0.3	50	10	10	60	0.15	0.2

non-flammable areas (e.g., buildings), non-uniform coverage with vegetation, and different values of τ_{ign} to demonstrate the performance of the algorithm. The fire front behaves qualitatively as expected in the presence of non-flammable areas, with the fronts eventually closing again in their wake. The timescale τ_{ign} affects S_f: if the ignition timescale is long, the front propagates slower. Further, if the coverage is low, fire may still propagate due to the long-distance transmission, but the front is more fragmented.

The model is demonstrated in more detail in Fig. 3, which is a zoomed-in snapshot from Fig. 2b. Unignited, ignited, and expired (i.e., decayed) particles are shown with the velocity vectors of the moving ones. It is evident that the present frame-

work enables the inclusion of very granular terrain information. Also, the combination of wind speed and turbulence (which determine the magnitude of the velocity), and the model's choice of parameters F_l, τ_{ign}, and τ_{mem} can determine the emergence of spot fires ahead of the main fire front and whether non-flammable areas will be overcome or not.

The above results are based on single realisations. By performing numerous realisations and by examining whether each cell at a particular instant ignited or not gives the probability that a particular location may burn. The variability between realisations depends on the problem and the terrain flammability inhomogeneity; therefore, no general statements can be made. For the problems presented in this Section, although each realisation
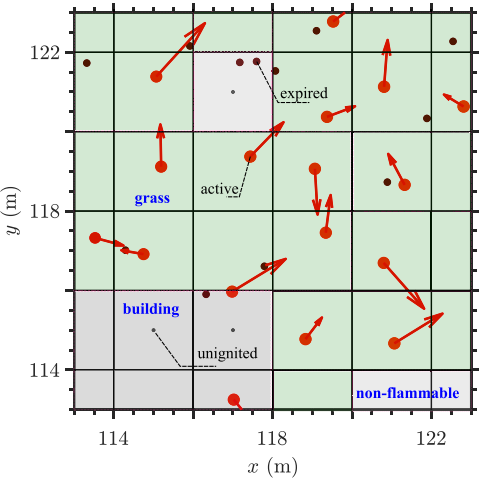
Fig. 3. Snapshot of the grid and the particles from Fig. 2b (northeast corner of the building at 2.5 mins). The locations of unignited, active and expired particles are shown together with the current velocity vectors of the active particles.

gives a different fire front, all the flammable cells away from large non-flammable regions got burnt in all realisations due to the large number of up-wind burning particles, as expected. However, the wake of a large non-flammable region, as in Fig. 2, can have a different spatial extent in each realisation.

From an assessment of the behaviour of the model for the above numerical experiments, we can conclude that the model can reproduce qualitatively many known features of fire behaviour in uniform and non-uniform terrain. The propagation speed, vegetation characteristics, the overall shape of the burnt area, and the effect of wind speed on the fire front propagation seem reasonably well captured.

3.2. Fire experiments with homogeneous vegetation

In this Section, an experimental fire [16,23,24] from a series of studies in Australia is modelled. In these experiments, uniform vegetation was used and the fire evolution was observed. The parameters used are given in Table 1, which includes some information from the experiments. The wind speed at 2 m height was 4.83 m/s, hence to extrapolate to 10 m a logarithmic velocity profile was used [25] to give $U_w = \ln(10/2) \times 4.83 = 7.7$ m/s. The observed fire speed and thickness were about 1.4 m/s and 10 m respectively. Here, $L_t = 10$ m because the dispersion is occurring at a lower height as the trees are shorter. The choice of $\tau_{ign} = 6.2$ s for this problem requires discussion, which could point to a way to systematise the selection of this input parameter. Gennaro et al. [16] discuss
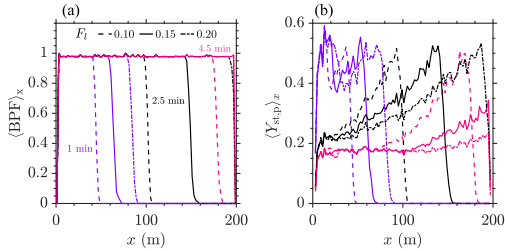

Fig. 4. Burn progress factor and ensemble-average particle status (averaged over the direction of the ignition line) at various times and choices of F_l for the Australian fire experiment. Parameters given in Table 1 unless otherwise indicated.

that for the type of tree in this experiment, 6.2 s is a reasonable estimate for the fire duration. Since our τ_{ign} in the present implementation of the model is the true ignition delay time plus the true burn time, we use the tree-specific burn time as the input τ_{ign} in our model. Note that for 5-m tall douglas fir trees a fire duration of 30 s has been measured [22]. For the Mati fire (see later), where the pine trees were much taller, a choice of a longer τ_{ign} (e.g., the 60 s used for Fig. 6) is hence partly justified.

Fig. 4 shows results for the Australian fire. In Ref. [16], the fire brush thickness is given as about 10 m. In our model, the fire front thickness can be defined in various ways. Here, we define it as the region where new ignitions are made and hence new particles are emerging. Using this definition, Fig. 4b shows a thickness of about 10–15 m. The fire front seems to maintain its structure. The choice $F_l = 0.15$ gives $S_f = 1.1$ m/s, which compares reasonably well with the experimentally observed value of 1.4 m/s. This case can also be used as a calibration for this constant and hence this value for F_l can be used for other problems too.

The sensitivity of the model to the values of the most important parameters is explored in Fig. 5, which plots the simulated S_f and front thickness δ_f for the indicated range of values for each of the model's input. It is clear that F_l, τ_{ign} and τ_{mem} are the most important parameters and their values affect S_f in the expected direction. For example, a larger F_l or smaller τ_{ign} cause an increase in S_f, while a long memory (higher τ_{mem}) causes a thickening of the fire front and an increase of its average speed. In future implementations of the model, physical sub-models can be used to distill detailed vegetation-specific information into single numerical values for these parameters. The number of particles emitted per cell and the cell size do not affect the propagation speed too much, implying a degree of grid convergence for the algorithm to these parameters. The front thickness is more sensitive to statistical convergence than the S_f, which is reasonably estimated even with one realisation for problems that have a statistically-homogeneous direction.
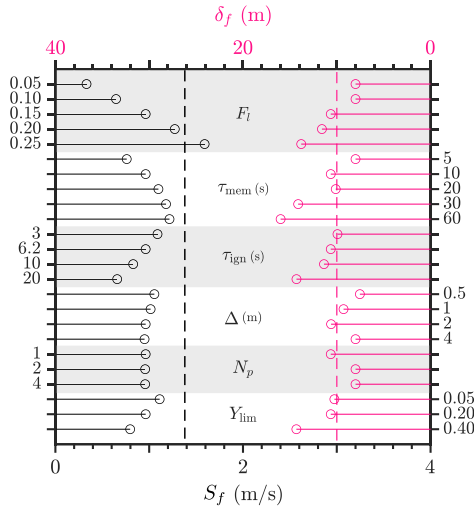
Fig. 5. Sensitivity of the model predictions for the fire front propagation speed (S_f; lower axis) and front thickness (δ_f; upper axis) to the various model parameters. For each parameter, the value used is marked and the length of the lines correspond to the resulting average S_f (left set of lines) and δ_f (right set of lines), the averaging being performed over the homogeneous direction. The experimentally observed values for the Australian fire experiments are denoted by the vertical dashed lines. The reference case about which the sensitivity analysis is performed is taken from Fig. 4 with $F_l = 0.15$. The sensitivity to radiation and to L_t is not significant for this problem.

3.3. Mati fire

On 23 July 2018, a devastating fire was initiated in a forest with pine trees in the west coast of Attica, Greece, and hit the seaside village Mati and the port of Rafina. The wind was West to East, 9–10 Beaufort scale, dry, and the temperature was 39°C. The fire descended a mountain slope, crossed a 25 m wide road located about 2 km from the sea shore to the East, and then entered the village composed of relatively regular plots of land with one- or two-storey detached houses. The majority of the plots included large pine trees (10–20 m tall) with full canopies and dry needles and debris. According to Ref. [27], the fire was of the crown type, the wind speed was about 90 km/hr (i.e., $U_w = 25$ m/s, with more accurate estimates from measurement stations giving an average 10-m wind speed of 19 m/s, with gusts reaching 25 m/s [28]), and the fire took about 50 mins to cover 3.4 km, resulting in an average propagation speed of about 1.1 m/s. Post-flame aerial views showed a very patchy behaviour, with many areas surviving while others getting completely burnt. Eye witnesses described flames that were very high and curved by the wind. Far-reaching ignitions, remote from actively burning trees, and fires going over houses were reported. Many survivors spoke of injuries caused by flying firebrands [28,29].

To model this WUI fire in the present framework, the parameters included in Table 1 were used. The flammable area is first represented using the Global PALSAR-2/PALSAR Forest/Non-Forest Map [26], embedded within the Google Earth Engine, that classifies the region in three distinct classes (Forest, Land and Water) using a high resolution of 25×25 m^2 per pixel at a pre-fire state. The Forest class is considered to be fully flammable, whereas 65% of the cells (randomly allocated) are assumed flammable for the Land class (brown shaded area in Fig. 6a) to account for the large pine trees in the village. The flammable ratio is estimated based on a regional average of the non-urban fabric as reported by Efthimiou et al. [29] and the 2018 Corine Land Cover (CLC) dataset [30]. Fig. 6b shows the fire front at an intermediate time. The burnt region outline is in good agreement with observation. The fire front reached the highway (Leof. Marathonos), marked by the dashed line in Fig. 6, in approximately 1 h following ignition, consistent with evidence [27]. At that time, the model
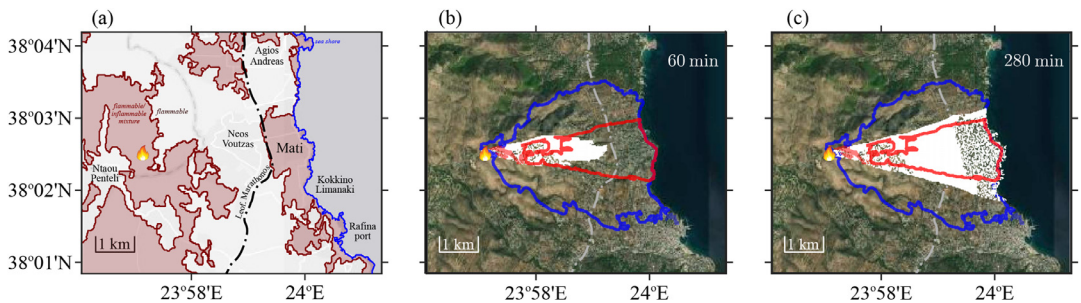

Fig. 6. (a) Regional map superimposed with brown-shaded areas denoting the built land [26], also containing large trees. Non-shaded land indicates dense forest. The thick blue line shows the sea shore. (b)-(c) Spread of the simulated fire, denoted by the white region, at the indicated time from ignition, overlayed on top of a satellite image. Thick lines: outline of the high fire intensity region (red) and the extent of the fire scar (blue), from post-fire satellite images. (For interpretation of the references to colour in this figure legend, the reader is referred to the web version of this article.)

gives a rate of fire speed of about 1 m/s, in good agreement with the observed speed (1.1 m/s). Note that the predicted S_f drops to about 0.65 m/s using $\tau_{ign} = 120$ s (see Supplementary Material), which may still be a reasonable time for the ignition delay plus the time to reach peak burn rate for a large dry pine tree. It is also evident that the fire crosses the highway and the urban area of Mati, enabled by the Lagrangian tracking of the convection fire particles and the finite "memory" imparted to them through the timescale τ_{mem}. Fig. 6c shows the final burnt region from the simulation. A fragmented front is predicted, consistent with eye witnesses. Due to the presence of plots of land that do not contain flammable material, neighbouring plots in their wake may survive the fire. This is consistent with a major observation from the Mati fire: houses and gardens downstream of plots without large pine trees were more likely to survive, while patches of large trees resulted in devastating consequences downstream. Such small-scale features of a wildland/urban interface fire can be captured with the proposed framework, given enough detail is supplied for each cell.

Concerning computational cost and considering only the run time, i.e., not including the user time to pre-process the satellite images needed to estimate values for τ_{ign} or to create the grid, the algorithm for the Mati fire can take of the order of a few seconds in a medium-performance laptop. This demonstrates that it can be developed as a real-time decision-support tool.

4. Further discussion and extensions

The presented algorithm should be considered as an extendable framework for modelling fire propagation and predicting the probability that a fire will hit a specific region. The proposed framework, by separating the "emitters" (i.e., the burning cells), the "bridge" (i.e., the wind, the radiation and the firebrands), and the "receivers" (i.e., the unburnt cells), allows attention to be focused on the individual physical processes active in each of these categories. Many physical phenomena of increasing complexity can be included. The various sub-models and parameters in the present model can be more tightly associated with the characteristics of the flammable material, the wind, the local fire front, and with any fire suppression strategies. Some examples follow.

A two-dimensional model was presented here, but the three-dimensional nature of the fire front can easily be captured by a 3D motion of the convection particles. The flames' height and any underlying distribution of flammability in the vertical direction can be included. Similarly for slope effects. In the present work, hot gases and firebrand random walk have been treated together, with their combined effect modelled by the parameters F_l and τ_{mem}; however, it is straightforward to separate these two and introduce separate random walks and "memory" timescales for the gases and the embers, with the latter also affected by gravity. The model's timescales can be more explicitly connected to the underlying physics of each of the subprocesses, such as ember combustion and lifetime, dilution by the cold wind, or ignition delay time of each cell. For instance, the decay timescale τ_{mem} can be explicitly evaluated by heat transfer or mixing analyses. The burning duration of a particular cell can be included through the number of particles emitted, while the fire intensity may be included through the initial $Y_{st,p}$. Similarly, typical firefighting actions such as temporally and spatially varying water deposition or the use of fire-breaks, may be incorporated into the model by dynamically changing the characteristics of the terrain or by acting on the $Y_{st,p}$ value of particles found within or emitted from a particular region. Real-time modifications to the cell flammability, i.e., the ignition delay time τ_{ign}, are also possible to account for clearing zones from vegetation and for unburnt cells that have received water or other fire extinguishing agents. Finally, fire-induced or building-induced modifications to the underlying fluid mechanical fields, such as dilatation-induced acceleration of the fire front and alterations of the turbulence or the streamline pattern, can be included through the parameters U_w, A, and L_t in the random walk.

5. Conclusions

A stochastic Lagrangian model based on the tracking of "virtual fire particles" has been proposed for simulating fire propagation in forests and the wildland-urban interface. The model treats fire propagation as a combination of radiative ignitions, a Langevin random walk due to the turbulent wind that simulates convection of hot gases and/or firebrands, and the emission of new "virtual fire particles" from flammable regions depending on their characteristics. The model aims for speed of execution while maintaining the key physics. It can give average and probabilistic information.

The results show that the model predicts reasonably well various known features of fire propagation. First, in the case of no wind and ignition from a point, the model gives a circular fire front, as expected. Second, non-flammable areas can be bypassed by the fire or flown-over due to a particular feature of the Lagrangian tracking used here where these "virtual fire particles" remain "live" according to a given timescale. Third, the average speed in homogeneous vegetation is of the order of 10–20% of the wind speed, as expected, and the exact ratio S_f/U_w depends mostly on the choice of the parameters F_l and τ_{ign}, which characterises the flammability of each cell. In non-uniform vegetation, where

flammable coverage is small, the fire speed is reduced and can even become zero.

The present model can be thought of as a framework, where improved knowledge or refined physical modelling of the individual sub-processes such as local flammability and burn rate, burn duration, height of flames, separate transmission through firebrands from hot gases, and fire- and building-induced flow changes can be included through the timescales of the algorithm. A data-driven approach to estimate these could also be explored [31]. The model can be used for calculating an average behaviour, but also as a Monte Carlo method to estimate burn probabilities of individual regions by an approaching fire. The model can be useful for evaluating mitigation strategies in a prevention or fire fighting sense.

Declaration of Competing Interest

The authors declare that they have no known competing financial interests or personal relationships that could have appeared to influence the work reported in this paper.

Acknowledgments

Supplementary material

Supplementary material associated with this article can be found, in the online version, at doi:10.1016/j.proci.2022.07.240

References

[1] D. Viegas, Forest fire propagation, Philos. Trans. R. Soc. Lond. 356 (1998) 2907–2928.

[2] D. Viegas, Overview of forest fire propagation research, in: Fire Safety Science – Proceedings of the Tenth International Symposium, 2011, pp. 95–108.

[3] M. Cruz, M. Alexandre, R. Wakimoto, Development and testing of models for predicting crown fire rate of spread in conifer forest stands, Can. J. Fores. Res. 35 (2005) 1626–1639.

[4] M. Alexander, M. Cruz, Evaluating a model for predicting crown fire rate of spread using wildfire observations, Can. J. Foresty Res. 36 (2006) 3015–3028.

[5] M. Cruz, M. Alexandre, The 10% wind speed rule of thumb for estimating a wildfire's forward rate of spread in forests and shrublands, Ann. For. Sci. 76 (2019) 44.

[6] D. Weise, B. Wotton, Wildland-urban interface fire behaviour and fire modelling in live fuels, Int. J. Wildland Fire 19 (2010) 149–152.

[7] H. Mahmoud, A. Chulahwat, Unraveling the complexity of wildland urban interface fires, Nat. Sci. Rep. 8 (2018) 9315.

[8] H. Mahmoud, A. Chulahwat, Assessing wildland - urban interface fire risk, R. Soc. Open Sci. 7 (2020) 201183.

[9] N. Liu, J. Lei, W. Gao, H. Chen, X. Xie, Combustion dynamics of large-scale wildfires, Proc. Combust. Inst. 38 (2021) 157–198.

[10] S. Manzello, S. Suzuki, M. Gollner, A. Fernandez-Pello, Role of firebrand combustion in large outdoor fire spread, Prog Energy Combust Sci 76 (2020) 100801.

[11] E. Ronchi, S. Gwynne, G. Rein, P. Intini, R. Wadhwani, An open multi-physics framework for modelling wildland-urban interface fire evacuations, Saf. Sci. 118 (2019) 868–880.

[12] A. Neophytou, E.S. Richardson, E. Mastorakos, Spark ignition of turbulent recirculating non-premixed gas and spray flames: a model for predicting ignition probability, Combust. Flame 159 (2012) 1503–1522.

[13] I. Karafyllidis, A. Thabailakis, A model for predicting forest fire spreading using cellular automata, Environ. Model. 99 (1997) 87–97.

[14] A. Collin, D. Bernardin, O. Sero-Guillaume, A physical-based cellular automaton model for forest-fire propagation, Combust. Sci. Technol. 183 (2011) 347–369.

[15] A. Trucchia, M. D'Andrea, F. Baghino, P. Fiorucci, L. Ferraris, D. Negro, A. Gollini, M. Severino, PROPAGATOR: an operational cellular-automata based wildfire simulator, Fire 3 (2020) 26.

[16] M. de Gennaro, Y. Billaud, Y. Pizzo, S. Garivait, J.-C. Loraud, M. El Hajj, B. Porterie, Real-time wildland fire spread modeling using tabulated flame properties, Fire Saf. J. 91 (2017) 872–881.

[17] Y. Liu, H. Liu, Y. Zhou, C. Sun, Spread vector induced cellular automata model for real-time crown fire behavior simulation, Environ. Model. Softw. 108 (2018) 14–39.

[18] J. Adou, A. Brou, B. Porterie, Modeling wildland fire propagation using a semi-physical network model, Case Stud. Fire Saf. 4 (2015) 11–18.

[19] S. Pope, Lagrangian PDF methods for turbulent flows, Annu. Rev. Fluid Mech. 26 (1994) 23–63.

[20] C. Anand, B. Shotorban, S. Mahalingam, Dispersion and deposition of firebrands in a turbulent boundary layer, Int. J. Multiph. Flow 109 (2018) 98–113.

[21] C. Rossa, P. Fernandes, Empirical modeling of fire spread rate in no-wind and no-slope conditions, Forest Sci. 64 (2018) 358–370.

[22] W. Mell, A. Maranghides, R. McDermott, S. Manzello, Numerical simulation and experiments of burning douglas fir trees, Combust. Flame 156 (2009) 2023–2041.

[23] N. Cheney, J. Gould, W. Catchpole, The influence of fuel, weather and fire shape variables on fire-spread in grasslands, Int. J. Wildland Fire 3 (1993) 31–44.

[24] N. Cheney, J. Gould, W. Catchpole, Prediction of fire spread in grasslands, Int. J. Wildland Fire 8 (1998) 1–13.

[25] C. Wiernga, Representative roughness parameters for homogeneous terrain, Bound. Layer Meteorol. 63 (1993) 323–363.

[26] M. Shimada, T. Itoh, T. Motooka, M. Watanabe, T. Shiraishi, R. Thapa, R. Lucas, New global forest/non-forest maps from ALOS PALSAR data (2007–2010), Remote Sens. Environ. 155 (2014) 13–31.

[27] E. Lekkas, P. Carydis, K. Lagouvardos, Mavroulis, S., M. Diakakis, E. Andreadadis, M. Gogou, N. Spyrou, M. Athanassiou, E. Kapourani, M. Arianoutsou, M. Vassilakis, P. Parcharidis, E. Kotsi, P. Speis, J. Delakouridis, D. Milios, V. Kotroni, T. Giannaros, S. Dafis, A. Karagiannidis, K. Papagiannaki, The July 2018 Attica (Central Greece) wildfires –scientific report (version 1.3), Newsletter of Environmental, Disaster, and Crisis Management Strategies 8 (2018).

[28] K. Lagouvardos, V. Kotroni, T. Giannaros, S. Dafis, Meteorological conditions conducive to the rapid spread of the deadly wildfire in Eastern Attica, Greece, Bull. Am. Meteorol. Soc. (2019) 2137–2145.

[29] N. Efthimiou, E. Psomiadis, P. Panagos, Fire severity and soil erosion susceptibility mapping using multi--temporal Earth Observation data: The case of Mati fatal wildfire in Eastern Attica, Greece, Catena 187 (2020) 104320.

[30] CLC, 2018, https://land.copernicus.eu/pan-european/corine-land-cover/clc2018.

[31] C. Zhang, M. Rochoux, W. Tang, M. Gollner, J.-B. Filippi, A. Trouvé, Evaluation of a data-driven wildland fire spread forecast model with spatially-distributed parameter estimation in simulations of the fireflux i field-scale experiment, Fire Saf. J. 91 (2017) 758–767.